

Technical Challenges and Performance of Satellite Communications on-the-Move Systems

Vijitha Weerackody and Enrique G. Cuevas

Satellite communications on-the-move (SOTM) terminals have become an essential component in military applications, primarily for tactical communications. SOTM terminals that are mounted on vehicles use very small antennas and consequently exhibit large beamwidths. Moreover, as the vehicle moves over rugged terrain, antenna-pointing errors may occur, thus causing potential interference to adjacent satellites. Although interference should be kept to a minimum, SOTM terminals must also transmit enough power to support broadband services with adequate data throughputs. These two conflicting demands present various technical and operational challenges. This article discusses considerations of the orbit and spectrum for the use of these terminals over geostationary satellites as well as considerations on antenna-pointing errors, effects of rain fading, and effects of interference on adjacent satellites.

INTRODUCTION

The growing demand from the commercial and military sectors for on-the-move communications at high data rates has generated interest in a new type of satellite terminal. These terminals can provide broadband communications from maritime vessels, trains, airplanes, land vehicles, and other transportation systems. Although the interest in the commercial sector is primarily in broadband Internet services, satellite communications on-the-move (SOTM) terminals have become an essential component in military applications, primar-

ily for tactical communications. Terminals mounted on land vehicles, also known as vehicle-mounted Earth stations (VMES), can provide two-way, high-data-rate services while on the move over geostationary satellites operating at the X, K_u , and K_a frequency bands. (The typical ranges of uplink and downlink frequencies used by satellites at the K_u -band are 14 and 12 GHz, respectively; the corresponding frequencies for the K_a -band are 30 and 20 GHz, and for the X-band are 8 and 7 GHz, respectively. A precise definition of the frequency bands

employed in satellite communications is given in Ref. 1.) VMES terminals generally consist of small high-performance antennas (aperture diameters from about 0.3 m to 1.0 m) and mechanical or electronic tracking systems with servo controllers and positioners, and the terminals can support vehicle speeds of up to about 100 km/h. The antenna size and other transmission parameters are selected to provide two-way communications under various terrain and operational conditions.

To achieve high data rates, VMES use high-efficiency parabolic antennas or phased-array antennas. However, as a consequence of the large beamwidth exhibited by antennas of this size, the effective isotropic radiated power (EIRP)—that is, the input power to the antenna multiplied by the antenna gain—that is transmitted from these terminals is limited by the main lobe rather than the side lobes, as is the case with larger-aperture antennas. This aspect is critically important for the operation of VMES, particularly when satellites are closely spaced along the geostationary arc, because this raises the potential for interference in the Earth-to-space as well as the space-to-Earth directions. Moreover, terminals in motion may cause additional interference to adjacent satellites because of potential antenna-pointing errors. Although we recognize that the interference generated toward adjacent satellites should be kept at a minimum, it is also essential that VMES terminals provide sufficient transmit power to support reasonable data rates required by broadband services. The studies performed by APL on this subject address these two conflicting demands: that is, how to ensure that the interference generated is acceptable to adjacent satellite system operators while at the same time providing an adequate EIRP spectral density (ESD) level that is acceptable to end users.

Recognizing the potential for widespread use of VMES and the need to protect existing services, regulatory and standards bodies such as the United States Federal Communications Commission (FCC),² the European Telecommunications Standards Institute (ETSI),³ and the International Telecommunications Union (ITU)⁴ have established regulations and technical requirements for the operation of VMES in the K_u -band.

In this article we address three aspects of the problem. First, we show that for small-aperture terminals, because of regulatory constraints on off-axis emissions, the spectral efficiency levels obtained from VMES links are low; hence, to support such low spectral efficiency levels, the modem of the VMES terminal should use efficient coding, modulation, and waveform spreading schemes. Second, the use of adaptive coding, modulation, and waveform spreading schemes is considered for mitigating the effects of rain fading; we show that these schemes can improve the spectral efficiency and performance of such links. Third, the impacts of motion-

induced antenna-pointing errors are discussed, and a statistical approach to limiting this type of interference is presented.

ORBITAL AND SPECTRUM CONSIDERATIONS

The broad coverage and reach offered by geostationary orbit satellites are attractive for VMES applications. The U.S. military, in particular, is currently interested in deploying systems at the X-band, K_u -band, and K_a -band.

X-Band

The X-band (7.9–8.4 GHz uplink/7.25–7.75 GHz downlink) is primarily used in the United States and other countries for military purposes. Currently there are about 45 satellites that operate in that band, and 60% of them are separated by 4° or more.

K_u -Band

The K_u -band (10.7–12.2 GHz uplink/14–14.5 GHz downlink) is used by satellite operators primarily for civilian commercial communications. This band is very attractive for enterprise and public networks because it allows the use of very-small-aperture terminals. However, because of bandwidth availability and global coverage, this band has also been used extensively in recent years to carry (nonprotected) military communications. Currently there are more than 230 satellites with K_u -band payloads.

K_a -Band

The K_a -band (24.75–25.25 and 27.5–29 GHz uplink/18.7–21.2 GHz downlink) is used primarily for civilian commercial communications, while the 30- to 31-GHz frequency band is used by some countries for military communications. Because the K_u -band has become congested, the K_a -band has become an attractive alternative, and many satellites are being planned in that band. However, this band suffers from significant rain attenuation losses that impact performance. Currently there are only 37 satellites with K_a -band payloads.

The U.S. Army plans to use SOTM terminals over DoD's Wideband Global Satellite Communications (WGS) satellites operating at X- and K_a -bands. The Project Manager Warfighter Information Network-Tactical (PM-WIN-T) also plans to use these terminals over commercial K_u -band satellites and is considering their use over the commercial K_a -band satellites.

Key Technical Challenges Encountered in VMES Systems

The interference paths to and from small-aperture-antenna terminals used in VMES terminals are shown

in Fig. 1. Here S_1 is the desired satellite and S_0 and S_2 are the adjacent satellites; T_1 and R_1 are the transmit and receive terminals that communicate with S_1 ; and T_0 and T_2 are the transmit terminals that are linked to S_0 and S_2 , respectively. All the terminals shown are small-aperture-antenna terminals. As shown in the figure, S_1 receives a significant level of uplink interference from T_0 and T_2 , and R_1 receives downlink interference from S_0 and S_2 . These interference paths significantly impact the link performance of the desired communication link $T_1S_1R_1$. Furthermore, to limit adjacent satellite interference from small-aperture-antenna terminals, the EIRP in the direction of adjacent satellites is restricted by regulatory and standards bodies. These restrictions effectively limit the radiated power and indirectly limit the data rates that can be supported.

Because VMES terminals are expected to operate satisfactorily in rugged terrain and at various vehicle speeds, motion-induced antenna-pointing errors are unavoidable. To maintain adequate antenna-pointing accuracy while operating in motion, VMES use motion-compensated antenna-tracking systems, which can be very expensive. Figure 2 shows the effects of these motion-induced antenna-pointing errors. In this figure the boresight of the antenna (defined as the direction of the antenna with the largest gain) is pointing away from the desired satellite, resulting in a reduction of the signal strength toward the satellite. More important, antenna mispointing increases the interference to adjacent satellites. Although reducing the EIRP of the antenna will mitigate this interference, this reduction also degrades the performance of the link. Thus, the challenge is to determine an EIRP level that keeps the interference to an acceptable level while ensuring that the link provides reasonable data rates. The recently issued recommendation of the ITU Radiocommunication Sector, ITU-R S.1857⁴ (developed by the authors of this article), addresses this problem by quantifying the interference as a function of the EIRP of the antenna and the statistics of the motion-induced antenna-pointing errors. Satellite service providers and operators can use the methodology provided in that recommendation to set the EIRP level of the VMES terminal so that the resulting interference corresponds to a mutually agreed-upon level.

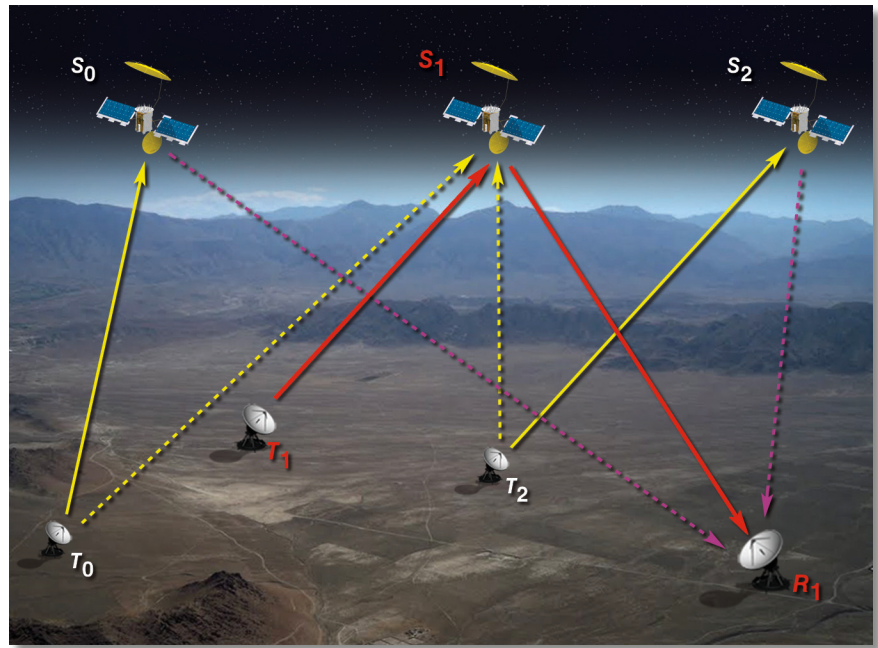


Figure 1. Uplink and downlink interference due to small-antenna-aperture terminals. S_1 is the desired satellite and S_0 and S_2 are the adjacent satellites; T_1 and R_1 are the transmit and receive terminals that communicate with S_1 ; and T_0 and T_2 are the transmit terminals that are linked to S_0 and S_2 , respectively.

SPECTRAL EFFICIENCY OBTAINED FROM K_u -BAND LINKS

The spectral efficiency, defined as the bit rate transmitted per unit bandwidth, is a key performance characteristic of a communication link. The link spectral efficiency η ($\text{bits}\cdot\text{s}^{-1}\cdot\text{Hz}^{-1}$) can be expressed in terms of the carrier-to-noise power ratio (C/N) and the bit energy-to-noise power spectral density ratio (E_b/N_0) at the receiver (Ref. 5):

$$\eta = \left(\frac{C/N}{E_b/N_0} \right). \quad (1)$$

Note that, in addition to the relationship shown in Eq. 1, E_b/N_0 is a function of η and depends on the particular coding and modulation scheme used in the communication link. The C/N ratio at the receiver can be expressed in terms of its uplink component $(C/N)_u$, downlink component $(C/N)_d$, and a component that accounts for interference (C/I) ; this interference component includes the total link interference and accounts for adjacent channel, adjacent satellite, and cross-polarization interference in the uplink and downlink directions. The $(C/N)_u$ term gives the carrier-to-noise power ratio for the link from the transmit terminal to the satellite receiver, and $(C/N)_d$ term gives the carrier-to-noise power ratio for the link from the satellite antenna output to the ground receiver. The overall (C/N) ratio is expressed as

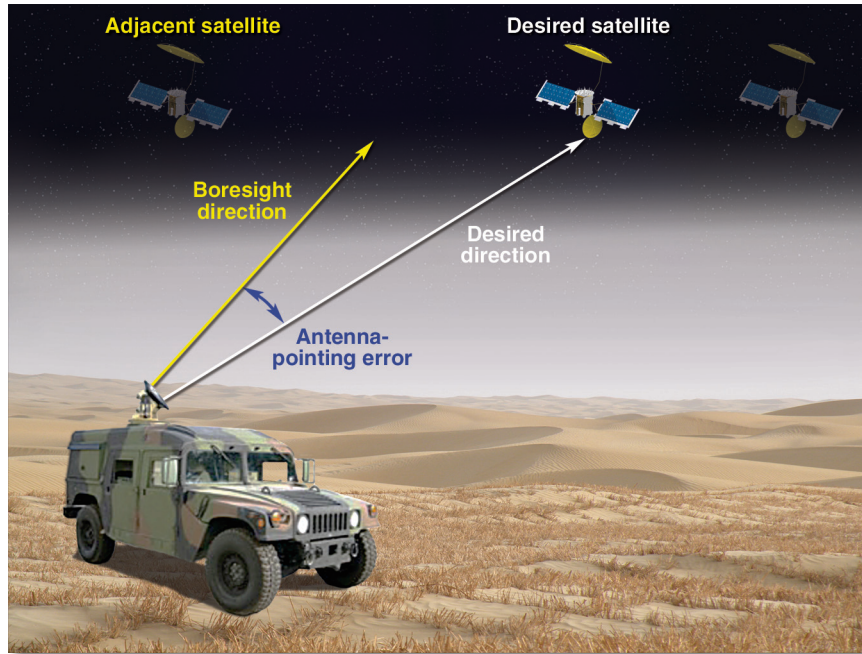


Figure 2. Boresight direction of the antenna pointing away from the desired satellite because of motion-induced antenna-pointing errors.

$$(C/N) = \left((C/N)_u^{-1} + (C/N)_d^{-1} + (C/I)^{-1} \right)^{-1}. \quad (2)$$

It can be seen that when one of the terms is significantly smaller than the others, that term dominates the overall C/N ratio and, hence, the link spectral efficiency. For a small-aperture-antenna VMES terminal, as discussed below, the EIRP from the antenna could be very small. This corresponds to a very small value for $(C/N)_u$. When a large-aperture antenna is employed at the receiver in the downlink, the corresponding values of $(C/N)_d$ and (C/I) could be very large. In this case, the aperture size of the VMES terminal is a key parameter that determines spectral efficiency of the link.

As noted in the *Key Technical Challenges Encountered in VMES Systems* section, to protect adjacent satellites from interference, regulatory and standards bodies have established limits on the EIRP that can be transmitted by a terminal in its off-axis direction. These off-axis emission limits impact the ESD that can be transmitted in the boresight direction from VMES terminals.

Figure 3 shows the off-axis emission limits as specified by recommendation ITU-R S.728-16 and the maximum ESD levels realized from antennas of aperture diameters 0.35, 0.5, and 0.6 m. The off-axis emission limits, also known as an ESD mask, start at 2° because this is the typical orbital separation between adjacent satellites in the K_u -band. The ESD patterns for the specific antennas are obtained by gradually increasing the power spectral density at the antenna input until the ESD at some off-axis angle just reaches its maximum limit. Because small antenna apertures have large beamwidths, it follows from

this figure that the off-axis emission limits reduce the boresight ESD from small-aperture antennas. For example, the difference in the boresight ESD between a 0.6-m antenna and a 0.35-m antenna is about 6.5 dB. When the overall link performance is dominated by the uplink, this corresponds to a nearly equal reduction in spectral efficiency for the smaller-aperture terminal, which is quite significant.

The spectral efficiency obtained for a satellite link that employs the Eutelsat W5 satellite is shown in Fig. 4. Here the transmit antenna is a VMES terminal with aperture sizes between 0.4 and 0.6 m, and the receiver terminal is stationary and represented by a large-aperture antenna. In this example, the overall performance of the link is dominated by the boresight ESD of the VMES terminal. As

noted earlier, the link spectral efficiency increases with the transmit antenna aperture size. Figure 4 shows the spectral efficiencies obtained when the coding, modulation, and waveform spreading schemes employed by the link correspond to the following: the theoretical Shannon capacity-achieving scheme; a hypothetical modem that gives an infinite number of rates for the combined coding, modulation, and waveform spreading scheme; and a practical modem obtained by quantizing the above hypothetical scheme using a rate 1/2 channel code with BPSK (binary phase shift keying) modulation and spread spectrum factors corresponding to 1, 2, 3, 4, etc.

The theoretical Shannon capacity-achieving results are computed by approximating the satellite link by an additive white Gaussian noise channel with its transmit power spectral density determined by the size of the terminal's antenna aperture. For the hypothetical coding, modulation, and waveform spreading scheme it is assumed that the relationship between the spectral efficiency and E_b/N_0 ratio is continuous with respect to the spectral efficiency, so any level of the spectral efficiency can be obtained using this mode. The practical coding, modulation, and waveform spreading scheme is obtained by quantizing the hypothetical scheme to a set of discrete levels of the spectral efficiency.

Consider the results shown in Fig. 4 for an antenna with an aperture diameter of 0.6 m. It can be seen that the theoretical Shannon capacity-achieving coding scheme can support a spectral efficiency of about $-1 \text{ dB}(\text{bits}\cdot\text{s}^{-1}\cdot\text{Hz}^{-1})$. This reduces to about $-5.2 \text{ dB}(\text{bits}\cdot\text{s}^{-1}\cdot\text{Hz}^{-1})$ for the hypothetical modem. The quantized spectral efficiency levels

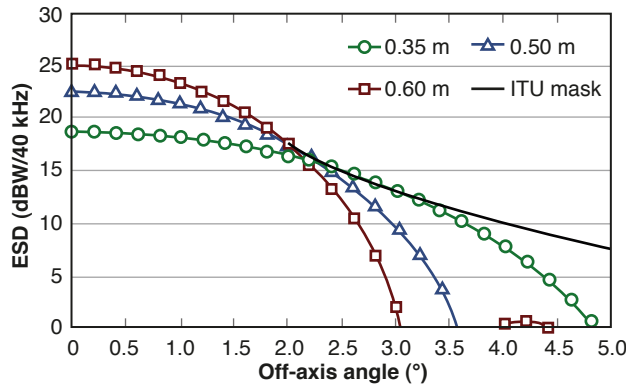


Figure 3. ESD as a function of the off-axis angle for antenna-aperture diameters of 0.35, 0.5, and 0.6 m (K_u -band).

for the practical modem are: -3.8 , -6.8 , -8.57 , -9.82 , and -10.79 $\text{dB}(\text{bits}\cdot\text{s}^{-1}\cdot\text{Hz}^{-1})$. These levels correspond to waveform spread factors of 1, 2, 3, 4, and 5 combined with a rate 1/2 channel code and BPSK modulation; they are shown in Table 1. It can be seen that the maximum spectral efficiency level that can be supported by this practical modem is -6.8 $\text{dB}(\text{bits}\cdot\text{s}^{-1}\cdot\text{Hz}^{-1})$. Next, consider the spectral efficiency results for a 0.4-m antenna aperture. The hypothetical modem gives a spectral efficiency of about -10.4 $\text{dB}(\text{bits}\cdot\text{s}^{-1}\cdot\text{Hz}^{-1})$. The maximum spectral efficiency obtained from the practical modem is -10.79 $\text{dB}(\text{bits}\cdot\text{s}^{-1}\cdot\text{Hz}^{-1})$, which corresponds to a waveform spread factor of 5.

Note that, because of off-axis emission limits, the transmit power spectral density is limited. Therefore,

Table 1. Quantized spectral efficiency levels obtained from a practical modem using combinations of different coding, modulation, and waveform spread factors.

Factor Combination		Spectral Efficiency, $\text{dB}(\text{bits}\cdot\text{s}^{-1}\cdot\text{Hz}^{-1})$
FEC Rate, Modulation Scheme	Waveform Spread Factor ^a	
3/4, 8PSK		2.73
3/4, 4PSK		0.97
2/3, 4PSK		0.45
1/2, 4PSK		-0.79
1/2, BPSK		-3.8
	2	-6.8
	3	-8.57
	4	-9.82
	5	-10.79
	6	-11.58
	7	-12.25
	9	-13.3
	13	-14.9
	16	-15.84

^aWith rate 1/2 FEC and BPSK.

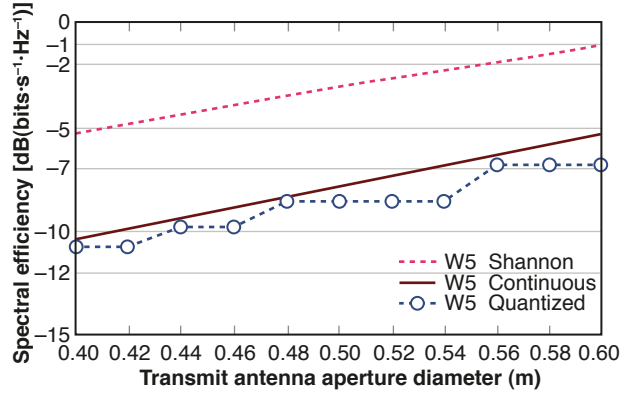


Figure 4. Spectral efficiency as a function of the diameter of the transmit antenna aperture for a typical K_u -band link.

the signal has to be spread so that the required amount of power can be transmitted to support the desired bit rate. In a VMES system, the link parameters may change dynamically depending on operational conditions. For example, the gain of the satellite antenna may vary by as much as 3–4 dB, and rain fading can degrade the signal by a similar amount. So the VMES terminal’s modem should be capable of supporting a large range of spectral efficiency values to accommodate these variable operational conditions. This can be achieved by using a combination of several waveform spread factors with different coding and modulation schemes.

SPECTRAL EFFICIENCY OBTAINED FROM K_a -BAND LINKS AND TECHNIQUES FOR MITIGATING RAIN FADING

The K_u -band satellites are heavily used, and the orbital spacing between satellites in this band is very small. On the other hand, existing and planned K_a -band satellites are located relatively far apart in the geostationary orbit. This makes them attractive for VMES applications. The off-axis emission mask applicable for the commercial K_a -band as established by recommendation ITU-R S.524-9⁷ is shown in Fig. 5. Note that, as shown in Figs. 3 and 5, both K_u - and K_a -band off-axis emission masks are applicable for off-axis angles more than 2° . It should be pointed out that a terminal’s ESD level has to comply not only with these off-axis emission masks but also with numerous interference requirements as discussed later in this article, under motion-induced antenna-pointing errors. So in the K_u -band, where the orbital spacing between the satellites is smaller, these interference requirements may dictate a smaller level for the terminal’s ESD.

Figure 5 also shows the maximum ESD patterns for antenna aperture diameters of 0.3, 0.35, and 0.4 m. The K_a -band transmit frequency is approximately twice the

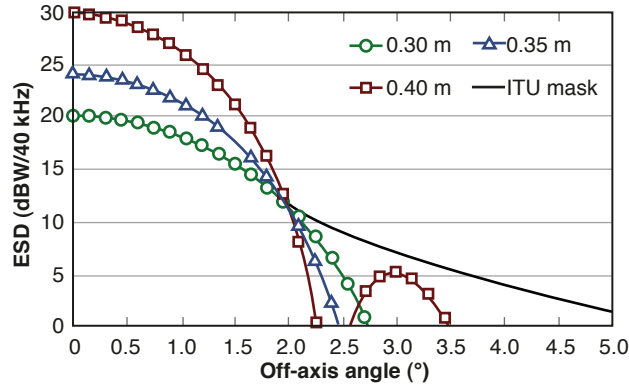


Figure 5. ESD as a function of the off-axis angle for antenna aperture diameters of 0.3, 0.35, and 0.4 m (K_a -band).

K_u -band frequency; therefore, the beamwidth at the K_a -band is approximately half the size of the corresponding K_u -band value. This narrower beamwidth of the antenna at K_a -band allows a larger boresight ESD from the antenna. However, this larger boresight ESD at the K_a -band is limited because, as seen from Figs. 3 and 5, the off-axis emission limits at the K_a -band are 6 dB below the corresponding K_u -band levels.

A key disadvantage of K_a -band operations is that rain attenuation at these frequencies is significantly more severe than at K_u -band frequencies. Therefore, appropriate measures should be taken to overcome the effects of rain fading. Satellite link performance under rain-fading conditions is stated in terms of a link availability level. For example, when the link is designed for a 99% annual availability level, link outages are expected to occur for an equivalent duration of 3.65 days of the year. A link outage refers to a case when some link metric, for example, the bit error rate, fails to meet its required threshold level.

Rain fading occurs in both uplink and downlink and, because of the higher uplink frequency range, rain fading is more severe in the uplink. Fortunately, using uplink power control techniques, it is easier to overcome the effects of rain fading in the uplink than in the downlink. The simplest approach to mitigating rain fading is to include a margin in the link design to guarantee the required link availability level. In conventional satellite links, which typically employ large-aperture antennas, this margin is achieved by temporarily transmitting at a higher ESD level than required under clear-sky conditions. In this case, under rain-fading conditions, the receiver has a sufficient carrier-to-noise power ratio to support the required bit rate. However, because large-aperture antenna terminals have very narrow antenna beamwidths, the off-axis emission limits will not constrain the transmit ESD. On the other hand, VMES terminals, because of off-axis emission limits, must transmit at the maximum allowed ESD under most operational conditions. Therefore, the required link

margin is achieved by transmitting the signal using a lower code rate or a larger waveform spread factor than required under clear-sky conditions. Thus, under clear-sky conditions the required bit rate is transmitted in a larger bandwidth than necessary.

This aspect is further illustrated using the results shown in Fig. 6, which shows the cumulative distribution function of the spectral efficiency obtained from a small-aperture-antenna (0.4-m diameter) VMES terminal operating from Miami, Florida, to Red Bank, New Jersey. The transmitter is a VMES terminal, and the receiver is a large-aperture terminal. Figure 6 shows the spectral efficiency under clear-sky and rain-fading conditions. The curves labeled “continuous” employ a hypothetical modem that supports unlimited levels of spectral efficiency, as discussed in the preceding section on spectral efficiency obtained from K_u -band links. The curve labeled “practical modem” employs a modem that supports quantized spectral efficiency levels of the hypothetical modem.

Satellite link parameters and the VMES terminal’s ESD are such that under clear-sky conditions, the spectral efficiency that can be supported by the link is about $3.65 \text{ dB}(\text{bits}\cdot\text{s}^{-1}\cdot\text{Hz}^{-1})$. (The off-axis emission mask for this case is set to 10 dB more than the off-axis emission mask specified by ITU-R S.524-97 and shown in Fig. 5.) However, under rain-fading conditions, the link spectral efficiency will be reduced. Suppose it is necessary to determine the spectral efficiency level that will guarantee a link availability of 99.5% for these link parameters. Figure 6 shows that for a 99.5% availability level, the spectral efficiency that can be supported by the link is $-5.48 \text{ dB}(\text{bits}\cdot\text{s}^{-1}\cdot\text{Hz}^{-1})$, or $1/3.53 \text{ bits}\cdot\text{s}^{-1}\cdot\text{Hz}^{-1}$. That is, the signal must be spread so that, in order to transmit a bit rate of $R_b \text{ bits/s}$, the bandwidth required is $3.53 \times R_b \text{ Hz}$. Conversely, to determine the link margin, the problem can be posed as follows: A link must be designed so that a spectral efficiency of $-5.48 \text{ dB}(\text{bits}\cdot\text{s}^{-1}\cdot\text{Hz}^{-1})$ is guaranteed for 99.5% of the time. What is the link margin, in terms of additional waveform spread factor, required under clear-sky conditions? From the above discussion the clear-sky spectral efficiency is $3.65 \text{ dB}(\text{bits}\cdot\text{s}^{-1}\cdot\text{Hz}^{-1})$ or $2.32 \text{ bits}\cdot\text{s}^{-1}\cdot\text{Hz}^{-1}$. That is, a bit rate of $R_b \text{ bits/s}$ needs a bandwidth of only $0.43 \times R_b \text{ Hz}$. However, to support the required availability level under rain-fading conditions, the corresponding bandwidth required is $3.53 \times R_b \text{ Hz}$. Therefore, the additional waveform spread factor under clear-sky conditions, which is the required link margin, is $10 \cdot \log(3.53/0.43)$ or 9.14 dB. Note that the link margin depends on the link parameters, required link availability, and the rain region.

Adaptive Coding, Modulation, and Waveform Spreading

The link margin technique to mitigate rain fading described above is spectrally very inefficient. An adap-

tive coding and modulation scheme can be used to improve the spectral efficiency, albeit at the expense of complexities associated with estimating the time-varying channel conditions. The adaptive coding and modulation scheme should support a large number of coding and modulation rates, so let us assume that a practical modem, which quantizes the spectral efficiency levels of the hypothetical modem discussed above, can be realized by the coding, modulation, and waveform spread factors shown in Table 1. This practical modem quantizes the spectral efficiency levels of the hypothetical modem to 14 levels, and these levels are shown in Fig. 6. (Note that the discrete spectral efficiency levels include a factor of 1.2 to account for waveform shaping.)

Consider the operation of the practical modem under gradually increasing rain-fading levels. As shown before, in clear-sky conditions the spectral efficiency supported by the link is $3.65 \text{ dB}(\text{bits}\cdot\text{s}^{-1}\cdot\text{Hz}^{-1})$. According to Table 1, the largest level of spectral efficiency smaller than this value that can be realized using the practical modem is $2.73 \text{ dB}(\text{bits}\cdot\text{s}^{-1}\cdot\text{Hz}^{-1})$. The practical modem operates using the corresponding coding and modulation scheme [rate 3/4 FEC (forward error correction) and 8PSK (phase shift keying)] until rain fading increases the signal attenuation resulting in the link spectral efficiency level falling below this value. The next smaller level supported by the practical modem is $0.97 \text{ dB}(\text{bits}\cdot\text{s}^{-1}\cdot\text{Hz}^{-1})$, which corresponds to a rate 3/4 FEC and 4PSK modulation. As the rain fading is gradually increased, the practical modem reduces its spectral efficiency levels as shown in Fig. 6. In comparison with the previously discussed link margin technique, the overall spectral efficiencies obtained from this adaptive coding and modulation scheme is very efficient. As can be seen from Fig. 6, the largest spectral efficiency, $2.73 \text{ dB}(\text{bits}\cdot\text{s}^{-1}\cdot\text{Hz}^{-1})$, occurs 92.7% of the time;

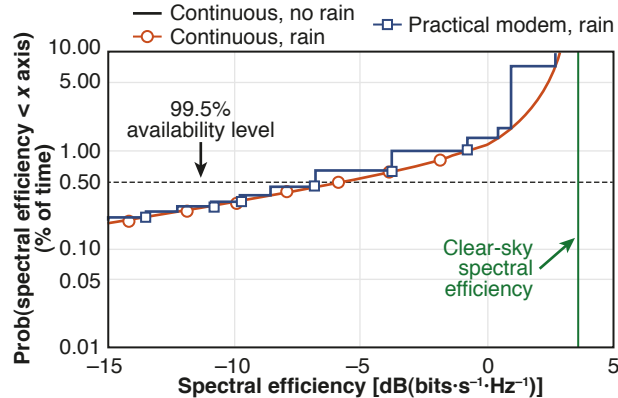


Figure 6. The cumulative distribution function of the spectral efficiency for a VMES link from Miami, Florida, to Red Bank, New Jersey, showing the following cases: clear-sky, hypothetical modem that supports continuous levels of spectral efficiency, and a practical modem that supports discrete levels of spectral efficiency.

the next, $0.97 \text{ dB}(\text{bits}\cdot\text{s}^{-1}\cdot\text{Hz}^{-1})$, occurs 0.4% of the time; $0.45 \text{ dB}(\text{bits}\cdot\text{s}^{-1}\cdot\text{Hz}^{-1})$ occurs 0.31% of the time; $-0.79 \text{ dB}(\text{bits}\cdot\text{s}^{-1}\cdot\text{Hz}^{-1})$ occurs 0.35% of the time; and smaller spectral efficiency values occur only for very small time periods. In this case the spectral efficiency obtained from the link is dynamic, with the spectral efficiency equal to or greater than $-15.84 \text{ dB}(\text{bits}\cdot\text{s}^{-1}\cdot\text{Hz}^{-1})$ for 99.8% of time. Note that, in the preceding link margin technique, the link spectral efficiency was fixed at $-5.48 \text{ dB}(\text{bits}\cdot\text{s}^{-1}\cdot\text{Hz}^{-1})$ for 99.5% of the time, and a link outage was declared for the remaining 0.5% of the time.

As previously mentioned, uplink power control is also a very useful technique for mitigating rain fading that occurs in the uplink. The off-axis ESD limits shown in Figs. 3 and 5 are applicable only for clear-sky conditions. When there is rain fading in the uplink, it is generally accepted that the ESD limits can be exceeded by an amount equal to the rain attenuation of the signal. The implementation of uplink power control requires careful design, because channel estimation errors could result in excess interference to adjacent satellites. Next-generation VMES terminals should combine all of the techniques described above to mitigate the detrimental effects of rain fading.

MOTION-INDUCED ANTENNA-POINTING ERRORS

Typically, VMES terminals are equipped with antenna-tracking mechanisms that attempt to maintain a reasonably small number of antenna-pointing errors. In rugged terrain conditions and at high mobile speeds, it is difficult to track the antenna and, consequently, the antenna-pointing errors may increase. Employing antenna-tracking devices that position the antenna precisely could be prohibitively expensive in many military and commercial applications. Therefore, motion-induced antenna-pointing errors are unavoidable with cost-effective VMES terminals. The off-axis emission masks shown in Figs. 3 and 5 have been established for stationary or static terminals. In the presence of motion-induced antenna-pointing errors, because the antenna boresight points toward off-axis directions, ESD from such an antenna may exceed its off-axis emission limits for short periods. Reducing the boresight ESD of the antenna can reduce the length and frequency of these times. However, in many operational environments, the amount of reduction in boresight ESD needed to satisfy the off-axis emission masks could be so large that the link can be rendered useless from a spectral efficiency standpoint. Therefore, the challenge here is to facilitate the use of VMES terminals that can operate at reasonable spectral efficiency levels while containing the interference to acceptable levels.

Traditionally, interference to other satellite networks is constrained using two criteria: specifying an off-axis emission mask (as discussed before) and limiting the

increase in the equivalent noise temperature at the victim receiver because of an interferer.⁸ Usually, the ESD from the transmit terminal has to satisfy both these criteria. In general, the off-axis emission mask dominates when the orbital distances between the desired satellite and its adjacent satellites are far apart, and limiting the increase in the equivalent noise temperature dominates when these orbital distances are very close. An effective interference-controlling method from VMES terminals should include aspects analogous to both criteria. Annexes 1 and 2 of ITU recommendation ITU-R S.1857⁴ address these two aspects in detail.

In the presence of motion-induced antenna-pointing errors, which can be considered random variables, the ESD in a given off-axis direction will vary with time. The variations of the ESD can be quantified using the underlying motion-induced antenna-pointing error random variables. Using this procedure, a statistical mask for the ESD can be obtained for VMES terminals. Specifically, a statistical ESD mask limits the probability that the ESD may exceed a corresponding reference ESD mask in some off-axis direction. Details of establishing a statistical ESD mask are given in Annex 1 of ITU recommendation ITU-R S.1857.⁴ In the following paragraphs, we present some salient features of such a statistical mask.

For example, the off-axis emission mask shown in Fig. 3 can be considered as the reference ESD mask. Figure 7 shows the maximum probability of ESD exceeding the sum of this off-axis emission mask and a parameter $EIRP_{\text{excess}}$, where the maximum is considered over all off-axis angles. Note that, because of motion-induced antenna-pointing errors, the instantaneous ESD may exceed the reference ESD mask, and $EIRP_{\text{excess}}$ is a parameter that represents the level of the instantaneous ESD above this reference ESD mask. Figure 7 shows five curves, each corresponding to a different motion-induced antenna-pointing error statistic. The statistical distributions of the motion-induced antenna-pointing errors are characterized by the parameters α and c , with α defining the tail of the distribution and c denoting a scale factor corresponding to the width of the probability density function. So, for the same value of α , a larger value of c corresponds to a larger motion-induced antenna-pointing error. Each curve is also labeled by E_B , which is the boresight ESD of the antenna corresponding to that plot. The E_B is determined as follows. Suppose the statistical ESD mask is as shown in this figure. Then, the motion-induced antenna-pointing errors are generated using the parameters α and c , and these antenna-pointing errors are fed to a given antenna. For this antenna configuration, the maximum probability of exceeding the sum of the reference ESD and $EIRP_{\text{excess}}$ is computed, where the maximum is calculated with respect to all off-axis angles, with E_B and $EIRP_{\text{excess}}$ as parameters. Starting from a very small value, E_B is

gradually increased until this maximum probability, for any value of $EIRP_{\text{excess}}$, reaches the corresponding value given by the statistical ESD mask. This is the maximum value of E_B that complies with the statistical ESD mask. The maximum probability corresponding to this E_B is shown in Fig. 7.

Note that the boresight ESD E_B obtained for the static case, that is in the absence of antenna-pointing errors and when using the reference ESD mask, is larger than its value that complies with the statistical ESD mask. Therefore, to accommodate the antenna-pointing errors in VMES terminals, the E_B has to be reduced from its static case value. A statistical ESD mask that allows the ESD to exceed the reference mask by a larger probability is indicated by the arrow for the lax mask in Fig. 7. Such a statistical ESD mask will result in a larger E_B , or a smaller reduction with respect to its static case value. The statistical ESD mask is useful because it accommodates expensive antenna systems, with precise pointing, with only a very small reduction in the E_B ; on the other hand, relatively less expensive antenna systems, which may allow larger pointing errors, may also be accommodated, albeit with a larger reduction in the E_B .

A key factor that determines the appropriate statistical ESD mask is the interference from the VMES terminal to other satellite networks. Annex 2 of recommendation ITU-R S.1857⁴ gives a detailed methodology to determine the boresight ESD level for a given level of link degradation at the victim receiver. When the E_B of the VMES terminal is determined according to both these annexes, the interference from these terminals can be effectively controlled.

CONCLUDING REMARKS

On-the-move communications is a new mode of communications that presents a new set of technical

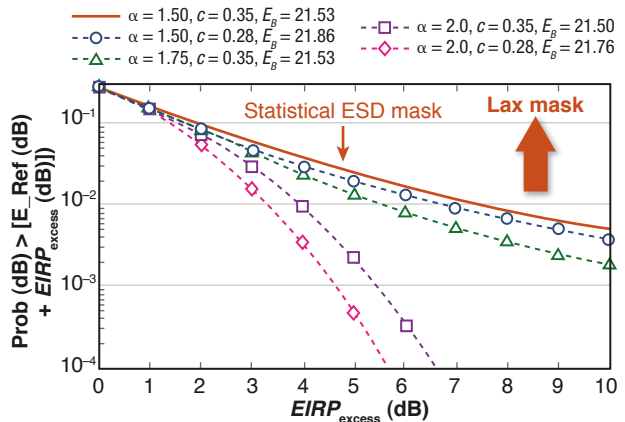


Figure 7. Probability of ESD exceeding the sum of a reference ESD mask and $EIRP_{\text{excess}}$.

challenges that need to be addressed. Conventional satellite communication systems consist of large, stationary antenna terminals that communicate on a link-to-link basis. A network of on-the-move terminals employs small antennas and uses multiple-access protocols to communicate among the terminals in the network. This article addresses some key aspects of on-the-move communications: link spectral efficiency and approaches to mitigating rain fading and motion-induced antenna-pointing errors. To develop an efficient on-the-move communications network for widespread use, further technical work is needed on issues such as quantifying interference, identifying protocols and techniques for optimizing limited satellite bandwidth and power resources, and the use of advanced signal processing for interference cancellation and mitigation. These issues are characteristic features of mature and advanced communication systems and are expected to be gradually introduced to on-the-move communication systems in the future.

ACKNOWLEDGMENTS: This work was supported by the United States Army (PM-WIN-T) in Aberdeen Proving Ground, Maryland, under Contract W15P7T-08-D-H412. Any opinions, findings, and conclusions or recommendations expressed in this material are those of the authors and do not necessarily reflect the view of the United States Army.

REFERENCES

- ¹Weerackody, V., and Gonzalez, L., "Mobile Small Aperture Satellite Terminals for Military Communications," *IEEE Commun. Mag.* **45**(10), 70–75 (2007).
- ²Federal Communications Commission, *Blanket Licensing Provisions for Domestic, U.S. Vehicle-Mounted Earth Stations (VMESs) Receiving in the 10.95–11.2 GHz (Space-to-Earth), 11.45–11.7 GHz (Space-to-Earth), and 11.7–12.2 GHz (Space-to-Earth) Frequency Bands and Transmitting in the 14.0–14.5 GHz (Earth-to-Space) Frequency Band, Operating with Geostationary Satellites in the Fixed-Satellite Service*, Report and Order FCC 09-64 (30 July 2009).
- ³European Telecommunications Standards Institute, *Satellite Earth Stations and Systems (SES); Harmonized EN for Vehicle-Mounted Earth Stations (VMES) Operating in the 14/12 GHz Frequency Bands Covering Essential Requirements Under Article 3.2 of the R&TTE*, Directive ETSI EN 302-977 (March 2010).
- ⁴International Telecommunication Union, *Methodologies to Estimate the Off-Axis E.I.R.P. Density Levels and to Assess Interference Toward Adjacent Satellites Resulting from Pointing Errors of Vehicle-Mounted Earth Stations in the 14 GHz Frequency Band*, Recommendation ITU-R S.1857 (2010).
- ⁵Weerackody, V., and Gonzalez, L., "Spectral Efficiency of Mobile VSAT Systems," in *Proc. IEEE Military Commun. Conf. (MILCOM 2007)*, Orlando, FL, pp. 1–7 (2008).
- ⁶International Telecommunication Union, *Maximum Permissible Level of Off-Axis E.I.R.P. Density from Very Small Aperture Terminals (VSATs)*, Recommendation ITU-R S.728-1 (1995).
- ⁷International Telecommunication Union, *Maximum Permissible Levels of Off-Axis E.I.R.P. Density From Earth Stations in Geostationary-Satellite Orbit Networks Operating in the Fixed-Satellite Service Transmitting in the 6 GHz 13 GHz, 14 GHz and 30 GHz Frequency Bands*, Recommendation ITU-R S.524-9 (2006).
- ⁸International Telecommunication Union, *Apportionment of the Allowable Error Performance Degradations to Fixed-Satellite Service (FSS) Hypothetical Reference Digital Paths Arising From Time Invariant Interference For Systems Operating Below 15 GHz*, Recommendation ITU-R S.1432 (2000).

The Authors



Vijitha
Weerackody



Enrique G.
Cuevas

Vijitha Weerackody is a member of APL's Principal Professional Staff and has extensive experience in research, development, and analysis of satellite and wireless communication systems. Dr. Weerackody also serves as an adjunct associate professor of electrical and systems engineering at the University of Pennsylvania, Philadelphia, Pennsylvania. **Enrique G. Cuevas** is a member of the APL Principal Professional Staff in the Network Management Systems Group in the Applied Information Systems Department. His current activities include the performance evaluation of the Internet Routing in Space (IRIS) system and interference studies of vehicle-mounted

Earth stations. He has been actively involved in the areas of satellite communication network technologies, performance and availability studies, and standards development for more than 20 years. For further information on the work reported here, contact Vijitha Weerackody. His e-mail address is vijitha.weerackody@jhuapl.edu.

The Johns Hopkins APL Technical Digest can be accessed electronically at www.jhuapl.edu/techdigest.